Conformational Study of Glycine Amide Using Density Functional Theory

Ping Li,[†] Yuxiang Bu,*[,†,‡] and Hongqi Ai[†]

Institute of Theoretical Chemistry, Shandong University, Jinan 250100, P. R. China, and Department of Chemistry, Qufu Normal University, Qufu 273165, P. R. China

Received: April 4, 2003; In Final Form: June 5, 2003

Seven stable stationary points, corresponding to three pairs of mirror-image conformers and one C_s symmetry conformer, have been located on the potential energy surface (PES) of neutral glycine amide at the B3LYP/6-311++G** level of theory. Accurate geometric structures, relative stabilities, and harmonic vibrational frequencies have been investigated. More importantly, the intramolecular H-bond formed from the amide to the amine plays a key role in stabilizing the global minimum, as observed in alanine amide and has been discussed qualitatively from the viewpoint of the structures, charge distributions, and vibrational analyses. As an important supplement in property for glycine amide, other property parameters, such as gas-phase basicity (GB), proton affinity (PA), and ionization potential (IP), have been predicted. The Boltzmann equilibrium distributions for the seven conformers have also been discussed qualitatively through the calculations of Gibbs free energy at various temperatures. At room temperature, the equilibrium compositions are mainly composed of conformers I and II exclusively, i.e., about 75.02% and 23.28%, respectively. As a tentative study, the conformational behaviors in aqueous solution have been explored using the Onsager model within the self-consistent reaction field (SCRF) method at the same level employed in the gas phase. Computational results indicate that the global minimum should be conformer I regardless of whether in the gas phase or in aqueous solution, which is different from the previous theoretical reports. Moreover, the consistent results in relative energy using higher-level computations, including the MP2, MP3, MP4SDQ, and CCSD(T) methods employing the Dunning's correlation consistent basis set aug-cc-PVDZ, indicate that the B3LYP/6-311++G** level of theory may be applied to the analogous systems.

1. Introduction

Glycine amide ($H_2NCH_2CONH_2$), being the simple derivative of glycine, is of great importance in the interstellar studies and biochemistry because amide derivates may also serve as simple models for N-terminal amino acids in peptides.[1] Obviously, the different conformations of glycine amide result from the rotating of three internal rotational degrees of freedom as for glycine, i.e., the rotation around C1−N4, C1−C2, and C2−N3 bonds displayed in Figure 1. In the gas phase, the existence of different conformers mainly derives from the delicate balances between stabilizing intramolecular H-bonds, destabilizing repulsive lone electron pairs, and steric effect. In solution, the extra interactions from the solvent molecules make the conformational behaviors more complex. As the simple amino acid, neutral glycine has been extensively studied by theoretical and experimental methods.[2−26] However, relatively little attention has been given to glycine amide. Experimentally, the lower thermal instability for glycine amide than glycine leads to more difficulties because it decomposes before melting. On the other hand, theoretical investigations based on various methods preclude the above difficulties and provide an alternative approach. On the basis of glycine amide, some related studies have been reported in the past.[27,28,30−34] For example, the formations of the peptide bond in glycine amide uncatalyzed or catalyzed by the metal cations or ammonia had been extensively studied.[27,28,30,31] Klassen et al. reported the collision-induced dissociation threshold energies of protonated glycine amide determined with a modified triple quadrupole mass spectrometer.[32] The interrelationship between conformations and theoretical chemical shift had been investigated by Sulzbach et al.,[33] in which some useful conformational information had been mentioned at the restricted Hatree−Fock (RHF) theory and 6-31G* basis set. Ramek et al. discussed the basis-set influence on the nature of the conformations of glycine amide (minimum or saddle point) in ab initio self-consistent field (SCF) calculations.[34] However, the detailed conformational analyses have not been investigated though some constructive suggestions may be obtained from above reports. On the other hand, the different conformations, especially for the global minimum, are indispensable to the calculations of proton affinities (PA), intrinsic gas-phase basicities (GB), and interactions with different mediums (such as metal cations), which are of fundamental importance in understanding the chemistry of peptides. To our best knowledge, the higher-level theoretical studies on the conformational analyses for glycine amide have not been reported to date, so it is necessary to carry out the present studies to lay the foundation for the future investigations.

Nowadays, density functional theory (DFT) has become a popular tool in computational chemistry increasingly. Not only does it include the electron corrections, but it is also computationally less expensive than the conventional electron corrections methods. What is more, it can provide many properties comparable in accuracy to experimental values and those obtained using *n*-order Møller−Plesset theory ($n = 2, 3, 4$) or even higher levels of ab initio methods. Many studies have shown that the nonlocal hybrid functional B3LYP method has been applied successfully to the medium-sized molecules.[20,23,29−31,36,37] A good case in point is that Barone

[†] Shandong University.
[‡] Qufu Normal University.

10.1021/jp034886f CCC: $25.00
Published on Web 07/31/2003

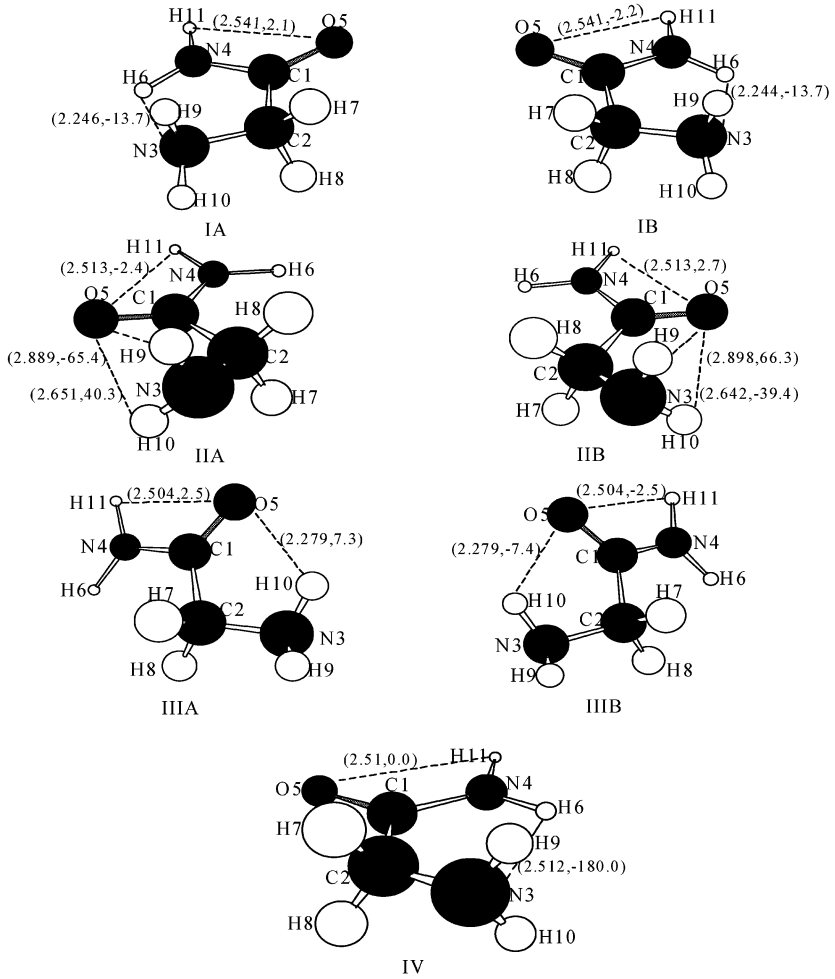

Figure 1. Conformers of glycine amide considered in this study. The data in parentheses refer to the H-bond distances and the dihedral angles formed among the two atoms forming the H-bond and other two atoms attached to the former, respectively.

et al.[12] have found that the B3LYP hybrid approach could give results close to the most sophisticated Hartree−Fock methods in a fraction of the computational time through the comparisons with the high-level results of Császár.[10] Additionally, the choice of basis set is crucial for obtaining the accurate results. The need for including diffuse and polarization functions in the basis set for calculations on hydrogen-bonded systems has long been recognized.[38,39] The basis set adopted here is 6-311++G**, which has been used by Császár to investigate the conformations of glycine and alanine conformers successfully.[10,13,29] The combination of B3LYP method with 6-311++G** basis set should give satisfactory results, as expected.

The goal of this study is to obtain accurate knowledge about the structural and conformational characteristics of glycine amide in the gas phase and in aqueous solution, to provide theoretical predictions, such as rotational constants, ionization potentials, and vibrational frequencies, which may be helpful to experimentalists. The gas-phase basicities (GB) and proton affinities (PA) have also been calculated on the basis of the accurate structures of the available conformers.

2. Computational Details

On the basis of the thirteen conformers of gaseous glycine studied by Császár,[10] all the possible geometries for glycine amide, where the −OH in glycine has been replaced by $-NH_2$ group, are fully optimized at the B3LYP/6-311++G** level of theory without any symmetry constraint. Every conformer is characterized by the harmonic frequencies using the analytical second derivative method and all the frequencies are unscaled in this paper.

As mentioned above, the density functional method adopted here is B3LYP, i.e., Becke's three-parameter hybrid functional using the Lee−Yang−Parr correlation function.[40,41] To further confirm the density functional results, single-point energy calculations have been performed by employing the higher-level calculations including second-, third-, and fourth-order Møller−Plesset theory (abbreviated as MP2, MP3 and MP4SDQ) and coupled cluster method (CCSD(T)) including the single, double, and perturbative triple excitation with the Dunning's correlation consistent basis set aug-cc-PVDZ. Only the valence electrons have been considered in the higher-level calculations mentioned above.

To evaluate the equilibrium distributions of all the available minima qualitatively, the relative Gibbs free energy has been calculated at various temperatures. The formula used can be described as follows:[8]

$$P_T(\mathrm{i}) = \frac{\mathrm{e}^{-\Delta G_T(\mathrm{i})/RT}}{\sum_{\mathrm{i}} \mathrm{e}^{-\Delta G_T(\mathrm{i})/RT}} \qquad (1)$$

where $\Delta G_T(\mathrm{i})$ is the Gibbs free energy of conformer i at temperature T relative to the global minimum, and R is the ideal gas constant.

To explore the conformational behaviors in aqueous solution qualitatively, the self-consistent reaction field (SCRF) method

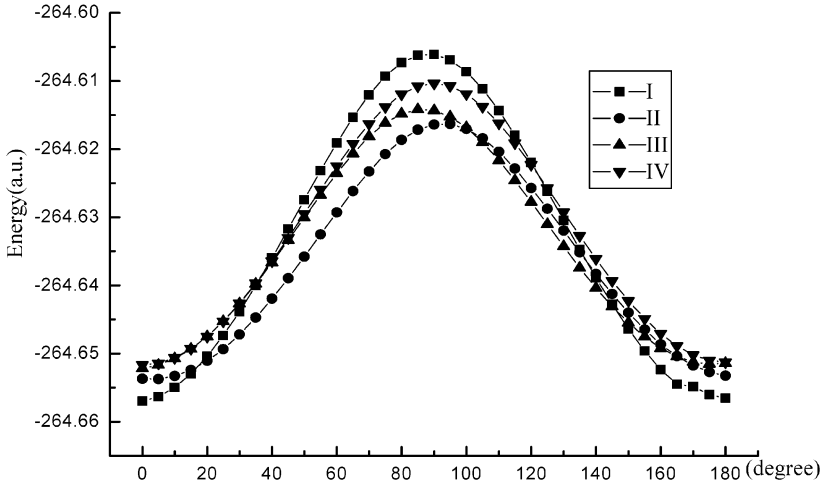

Figure 2. Dependence of the PES on the rotation of NH_2-amide group along the C1−N4 bond.

was carried out on the basis of the Onsager model.[43−46] As usual, the solvent is viewed as a continuous dielectric medium characterized by a uniform dielectric constant (ϵ) in this model ($\epsilon = 78.39$ for water). The solute occupies a spherical cavity inside the solvent. The permanent dipole moment of the solute induces a dipole moment (reaction field) in the surrounding medium, which in turn will interact with the dipole moment of the solute. This solute−solvent interaction is updated until self-consistency is achieved. The initial geometries start form the optimized gas-phase structures. The predicted radius can be obtained from the volume calculations based on the gas-phase geometries.

For the following protonation process, i.e., $B + H^+ \rightarrow BH^+$, the enthalpy changes and Gibbs free energy changes can be calculated as[37]

$$\Delta H = E(BH^+) - E(B) - E(H^+) + \Delta(PV)$$
$$= E(BH^+) - E(B) + E_{vib}(BH^+) - E_{vib}(B) - 2.5RT \quad (2)$$

$$\Delta G = \Delta H - T\Delta S \qquad (\Delta S = S(BH^+) - S(B) - S(H^+)) \quad (3)$$

where the E(i), E_{vib}(i), and S(i) refer to the total energy, zero-point vibrational energy (ZPVE) and entropy of the species i. As a rule, GB and PA are defined as the negative of the Gibbs free energy changes and enthalpy changes, i.e., $GB = -\Delta G$, $PA = -\Delta H$, respectively. To eliminate the basis set superposition errors (BSSE) produced in the calculations of GB and PA, the Boys−Bernardi counterpoise technique[42] has been used.

All the computations were performed using the Gaussian98 program and the SCF convergence criteria *Tight* have been used throughout the calculations.[47]

3. Results and Discussions

Geometric parameters, dipole moments and rotational constants of the seven conformers are first listed in Table 1, which can be classified as four types of conformations approximately in term of their structural features (see Figure 1), i.e., IA-IB, IIA-IIB, IIIA-IIIB, and IV conformers, respectively. For the sake of simplicity, the symbol I stands for mirror-image conformer IA and IB and the same holds for II and III if not noted otherwise. Additionally, we only take conformer IB, IIB, IIIB, and IV, for instance, because the mirror-image conformers are identical to each other in energy and in structural parameters except for the dihedral angles. For comparison, the structural parameters in aqueous solution are also presented in Table 2. The energy quantities, such as total energies, relative energies and zero-point vibrational energies, are summarized in Table 3. Calculated GBs and PAs are given in Table 4. Tables 5 and 6 list the charge distributions and calculated IPs, respectively. Vibrational frequencies, infrared intensity, and the descriptions of the normal modes are presented in Table 7. Figure 2 shows the dependence of the PES on the rotation of NH_2 amide group along the C1−N4 bond. Finally, the dependences of the equilibrium distributions, entropy, and enthalpy on temperatures for the seven conformers are depicted in Figures 3−5, respectively.

3.1. Geometries. Full geometry optimizations reveal that there are seven stable stationary points (see Figure 1), which correspond to seven different conformers on the potential energy surface (PES) of glycine amide. Their corresponding structural parameters, including bond lengths, bond angles, and dihedral angles, are listed in Table 1. As mentioned in the second section, they can be classified as four types of conformers according to their structural similarities. Obviously, three pairs of conformers, i.e., IA-IB, IIA-IIB, and IIIA-IIIB conformers, possess mirror-image features and conformer IV is the only one that possesses the C_s symmetry.

Inspections of the data listed in Table 1 suggest that the bond lengths have no substantial changes for all the conformers; for example, the largest deviations for the distance between C2 and N3 (designated as C2−N3; see Figure 1) are 0.0172 and 0.0096 Å for C1−N4 and 0.0058 Å for C1−C2, respectively. To investigate the nature of the peptide bond (C1−N4), another two molecules, i.e., H_3C-NH_2 and $H_2C=NH$, have been optimized at the same level of theory employed above. Compared with them, the bond length and electron density between C1 and N4 lie between those of H_3C-NH_2 (single C−N bond) and $H_2C=NH$ (double C=N bond), indicating that the C1−N4 peptide bond possesses partial double bond characteristics. This bond length is also well consistent with the peptide bonds in di- and triglycine and experimental results.[21,48] Similarly, the partial C=O double bond character in the peptide group has also been observed because its bond length and electron density lie between those of methanol (H_3C-OH) and acetone ($(CH_3)_2C=O$) optimized at the same level. As a result, the C=O bond length is larger than those of glycine and alanine (by about 0.01 Å).[10,13,29] Considering that the formation of an H-bond may be reflected from the distance, the possible intramolecular H-bonds given in Figure 1 can be assessed by the distance between the proton donor and acceptor. The short distance has implied that the H-bond formed from the amide to the amine in conformer

TABLE 1: Selected Geometric Parameters, Rotational Constants and Dipole Moments of Glycine Amide and Alanine Amide[a]

parameter	IB	IIB	IIIB	IV
R(C1C2)	1.5338 (1.53)	1.5396	1.5281 (1.53)	1.5379
R(C2N3)	1.4673 (1.46)	1.4501	1.4559 (1.45)	1.4536
R(C1N4)	1.3566 (1.36)	1.3662	1.3640 (1.37)	1.3634
R(C1O5)	1.2198 (1.22)	1.2175	1.2181 (1.22)	1.2186
R(N4H6)	1.0097 (1.00)	1.0065	1.0061 (1.00)	1.0057
R(N3H9)	1.0142 (1.01)	1.0151	1.0126 (1.01)	1.0115
R(N3H10)	1.0127 (1.01)	1.0155	1.0165 (1.00)	1.0115
R(N4H11)	1.0072 (1.00)	1.0083	1.0084 (1.00)	1.008
A(C1C2N3)	113.67 (111.4)	115.40	109.73 (112.5) (106.8)	120.66
A(C2C1N4)	114.68 (114.1)	114.98	115.47 (115.3) (116.3)	116.77
A(C2C1O5)	120.94 (121.2)	122.41	121.77 (121.7) (121.1)	120.43
A(C1N4H6)	118.97 (117.6)	122.36	122.02 (119.8) (119.6)	122.02
A(C2N3H9)	111.53 (109.3)	110.21	111.55 (108.0) (108.9)	114.37
A(C2N3H10)	111.57 (108.8)	109.71	108.99 (106.0) (107.0)	114.37
A(C1N4H11)	119.29 (117.3)	118.82	118.33 (116.6) (114.7)	118.60
A(H9N3H10)	107.43 (105.7)	105.77	108.63 (103.7) (106.7)	110.81
A(H6N4H11)	121.58 (120.5)	118.72	118.73 (117.2) (116.4)	119.38
D(C2C1N4H6)	1.09/−1.01	−0.09/−0.11	11.64/−11.70	0.00
D(C2C1N4H11)	176.69/−176.72	−176.43/176.80	−179.50/179.56	180.00
D(C1C2N3H9)	88.63/−88.58	63.86/−63.44	−153.72/153.47	64.65
D(C1C2N3H10)	−151.22/151.28	−52.22/52.66	−33.77/33.48	−64.65
D(N3C2C1N4)	13.84 (13.6)/−13.93	−170.50/171.09	−153.14 (−151.4)/153.33 (151.2)	0.00
D(N3C2C1O5)	−167.23 (−166.9)/167.15	10.37/−9.72	29.83 (28.7)/−29.60 (−34.0)	180.00
D(N4C1C2H7)	141.07 (137.6)/−141.17	67.69/−67.03	83.39 (87.8)/−83.20 (−88.4)	124.15
D(N4C1C2H8)	−105.67 (−106.6)/105.57	−47.02/47.66	−31.60 (−31.1)/31.79 (29.6)	−124.15
A[b]	9.629 (3.32)	10.030 (−3.3)	9.945 (1.08)	9.500 (4.16)
B	3.963 (−0.34)	3.824 (0.73)	3.928 (−3.44)	3.879 (0.00)
C	2.916 (2.34)	2.867 (−0.33)	2.939 (0.96)	2.846 (0.42)
dipole moment[c]	4.07 (5.37)	3.44 (4.80)	3.73 (4.82)	4.18 (5.13)

[a] The structural parameters in parentheses refer to the results of alanine amide optimized at the MP2/6-31+G** level from ref 1 and all the bond lengths (*R*), bond angles (*A*), and dihedral angles (*D*) are in angstroms and degrees, respectively. The data behind the slash refer to the structural parameters of its corresponding mirror-image conformers. [b] Rotational constants (*A*, *B*, *C*) are in GHz, and the data in parentheses refer to the dipole moments (in Debye) along the principal axes. [c] The data in parentheses refer to the dipole moments in aqueous solution.

I is stronger than that in conformer IV (2.24 vs 2.51 Å). Another kind of H-bond may be found in conformer III between the carbonyl oxygen and the hydrogen of the amine NH_2 group. Many studies have demonstrated that the NH_2 is a good proton acceptor but a less effective proton donor,[11,12,20] so the strength of H-bond in conformer III should be less than that in conformer I. Obviously, the large distances between the carbonyl oxygen and two hydrogen atoms in amine NH_2 show that the existence of H-bond in conformer II is impossible and the dihedral angles of the four atoms (see Figure 1) also disfavor the formation of H-bond. The distance between H11 and O5 in every conformer, being slightly smaller than the sum of the van der Waals radius of the two atoms (about 2.6 Å), suggests that the strength of H-bond formed between them is small on the assumption that H-bond could be formed though we are hesitant to impute the H-bond properties to it in this paper. Additionally, the different bond length in the NH_2 group also results from the intramolecular H-bond influence. For example, the length of N4—H6 is larger than that of the N4—H11 in conformer I because the strength of H-bond formed from the amide to the amine is larger than that of the carbonyl oxygen O5 with H11 in amide.

As far as the bond angles are concerned, the deviations among the seven conformers are larger with respect to those of the bond lengths. The largest deviation among all the conformers is the *A*(C1C2N3), which is up to 6.99°, and the others are no more than 2°. These results can be comparable to the corresponding parameters of formamide and alanine amide.[1,49]

For the dihedral angles, the negative and corresponding positive angles may reflect the mirror-image features for the mirror-image conformers. Most importantly, the planarity of the peptide bond has been reproduced in glycine amide, as can been seen from Table 1. The dependence of the PES on the rotation of the NH_2 amide group along the peptide bond depicted in Figure 2 should also give another support for the planarity of the peptide bond. As discussed below the conformer IV with C_s symmetry is 12.39 kJ/mol higher in energy than the global minimum, so the conclusions may be drawn that the conformations with slightly nonplanar peptide bonds can be more stable than the fully planar geometry, which are consistent with the results of diglycine, triglycine, and alanine dipeptide.[21]

It is interesting to compare the results of conformations with other reports where possible. Sulzbach et al. mentioned that the global minimum for glycine amide should be located at 165.0° for *D*(N3C2C1N4) (see Figure 1), in which the two hydrogens bound to the amino nitrogen form H-bonds of a different length with the carbonyl oxygen.[33] On the contrary, this conformer corresponds to the conformer IIB in present study, which is 6.28 kJ/mol higher in energy than the global minimum. Because there are no experimental results available, we can compare our results with the analogous molecule alanine amide. It is reported that the introduction of the methyl group for α−alanine with R = CH_3 to replace one of the hydrogens of glycine (R = H) has a rather small effect on either the geometry or conformational preference of α-alanine.[13,29] By analogy, we think the results of glycine amide should be analogous to those of alanine amide. From the selected structural parameters (especially for dihedral angles) of alanine amide listed in Table 1, we can see that the geometries of glycine amide may be comparable to those of alanine amide,[1] i.e., the global minimum of glycine amide corresponds to the global one for alanine amide and the conformers IIIA and IIIB correspond to the other two minima of alanine amide, respectively. If we optimize the structure in which one of the hydrogens (H7 or H8) is replaced by R = CH_3 in the C_s symmetry structure IV, a new stable alanine amide conformer can still be obtained at the B3LYP/6-311++G** level of theory, which has not been mentioned previously.[1] Thus

TABLE 2: Structural Parameters of Glycine Amide in Aqueous Solution[a,b,c]

parameter	IB	IIB	IIIB	IV
R(C1C2)	1.5366 (0.003)	1.5375 (−0.002)	1.5276 (−0.001)	1.5396 (0.002)
R(C2N3)	1.4614 (−0.006)	1.4591 (0.009)	1.4589 (0.003)	1.4475 (−0.006)
R(C1N4)	1.3493 (−0.007)	1.3554 (−0.011)	1.3595 (−0.005)	1.3548 (−0.009)
R(C1O5)	1.2281 (0.008)	1.2247 (0.007)	1.2225 (0.004)	1.2252 (0.007)
R(N4H6)	1.0133 (0.004)	1.0076 (0.001)	1.0076 (0.002)	1.0071 (0.001)
R(C2H7)	1.0956 (0.0)	1.097 (0.0)	1.1018 (−0.001)	1.0942 (0.001)
R(C2H8)	1.0937 (0.0)	1.0928 (−0.002)	1.0948 (−0.001)	1.0942 (0.001)
R(N3H9)	1.0129 (−0.001)	1.0154 (0.0)	1.013 (0.0)	1.0110 (−0.001)
R(N3H10)	1.0119 (0.0)	1.0175 (0.002)	1.0164 (0.0)	1.0110 (−0.001)
R(N4H11)	1.0064 (0.0)	1.009 (0.0)	1.0082 (0.0)	1.0081 (0.0)
A(C1C2N3)	113.48 (−0.193)	113.69 (−1.71)	110.09 (0.36)	121.15 (0.49)
A(C2C1N4)	114.10 (−0.580)	115.88 (0.90)	115.23 (−0.24)	116.65 (−0.12)
A(C2C1O5)	121.38 (0.439)	120.97 (−1.44)	121.92 (0.15)	120.04 (−0.39)
A(C1N4H6)	117.99 (−0.98)	122.47 (0.11)	122.05 (0.03)	121.70 (−0.32)
A(C1C2H7)	106.58 (0.0)	106.56 (−0.84)	105.93 (0.39)	105.44 (−0.33)
A(C1C2H8)	105.85 (−0.02)	110.94 (1.72)	109.70 (−0.40)	105.44 (−0.33)
A(C2N3H9)	112.83 (1.30)	109.52 (−0.69)	110.87 (−0.68)	115.37 (1.00)
A(C2N3H10)	112.90 (1.33)	107.77 (−1.94)	108.53 (−0.46)	115.37 (1.00)
A(C1N4H11)	120.23 (0.94)	119.33 (0.51)	118.69 (0.36)	119.37 (0.77)
A(H7C2H8)	106.29 (−0.33)	106.32 (0.16)	106.80 (−0.05)	105.64 (0.06)
A(H9N3H10)	107.78 (0.35)	105.97 (0.20)	108.76 (0.13)	111.09 (0.28)
A(H6N4H11)	121.78 (0.20)	118.16 (−0.56)	118.23 (−0.50)	118.93 (−0.45)
D(N3C2C1N4)	7.84/−9.07 (−6.00)	−159.56/160.36 (10.94)	−159.67/160.19 (−6.53)	0.0 (0.0)
D(N3C2C1O5)	−172.98/171.87 (−5.75)	22.74/−21.86 (12.37)	21.69/−21.13 (−8.14)	180.0 (0.0)
D(C2C1N4H6)	−0.36/0.33 (−1.45)	5.25/−4.75 (5.34)	−2.86/3.33 (−14.50)	0.0 (0.0)
D(C2C1N4H11)	179.06/−178.76 (2.37)	−77.10/176.85 (−0.67)	−171.02/170.68 (8.48)	180.0 (0.0)
D(N4C1C2H7)	134.20/−135.70 (−6.87)	79.95/−79.05 (12.26)	76.79/−76.27 (−6.60)	124.26 (0.11)
D(N4C1C2H8)	−112.93/111.39 (−7.26)	−35.37/36.22 (11.65)	−38.14/38.66 (−6.54)	−124.26 (−0.11)
D(C1C2N3H9)	100.95/−98.51 (12.32)	79.41/−77.27 (15.55)	−153.19/153.36 (0.53)	65.87 (1.22)
D(C1C2N3H10)	−136.53/139.34 (14.69)	−35.43/37.66 (16.79)	−33.80/34.05 (−0.03)	−65.87 (−1.22)

[a] The units used here are identical to those in Table 1. [b] The data in parentheses refer to the structural changes from gas-phase to aqueous solution. [c] The data behind the slash refer to the structural parameters of its corresponding mirror-image conformers.

TABLE 3: Total Energies (au), Relative Energies (kJ/mol), and ZPVE (kJ/mol) of Glycine Amide Conformers at B3LYP/6-311++G Level**

	IB	IIB	IIIB	IV
E_{total}	−264.6571001	−264.6537941	−264.6522276	−264.6516886
ZPVE	241.25	238.85	239.43	239.44
$\Delta E_{relative}$[a]	0.0 (0.0)	8.68 (6.28)	12.80 (10.97)	14.21 (12.39)
MP2[b]	−263.884547 (0.0)	−263.8816296 (7.64)	−263.8803353 (11.04)	−263.8791704 (14.10)
MP3[b]	−263.9086744 (0.0)	−263.9063481 (6.05)	−263.9048673 (9.94)	−263.903447 (13.67)
MP4SDQ[b]	−263.9202954 (0.0)	−263.9179322 (6.15)	−263.9164657 (10.00)	−263.9150942 (13.60)
CCSD (T)[b]	−263.9503204 (0.0)	−263.9477519 (6.63)	−263.9463463 (10.32)	−263.9449976 (13.86)
$E_{aqueous}$[c]	−264.6629221 (0.0)	−264.6580681 (9.69)	−264.6561156 (14.29)	−264.6565844 (12.63)
$\Delta E_{solution}$[d]	−15.29	−11.22	−10.21	−12.85

[a] The data in parentheses refer to the relative energies including ZPVE corrections. [b] The single-point energy calculations using the aug-cc-PVDZ basis set based on the optimized structures at the B3LYP/6-311++G** level, the data in parentheses refer to the relative energies with respect to IB (in kJ/mol). [c] The total energies of the conformers in aqueous solution and the relative energies in parentheses (including ZPVE corrections) with respect to IB at the B3LYP/6-311++G** level. [d] The data refer to the solvation energy (in kJ/mol).

the analogy mentioned above is also true between glycine amide and alanine amide.

In aqueous solution, the conformations of I, II, and III remain practically unaltered except for the dihedral angles with respect to the geometries in the gas phase. At the same time, conformer IV still keeps the C_s symmetry and has almost no changes in structural parameters. Obviously, the mirror-image conformers in the gas phase also assume the same relationships in aqueous solution as listed in Table 2.Table 1 also presents the rotational constants and dipole moments of all the conformers. Obviously, the dipole moments in aqueous solution are larger than those in the gas phase. The large dipole moments may be helpful in the observation of the conformers using the microwave spectrum because the microwave transition intensities are proportional to the square of the dipole moments. Another point is that the large dipole moments should result in an extra stabilization in aqueous solution, which can be supported by the following discussions. Additionally, the calculated rotational constants should be helpful in the search for these conformers using the rotational spectroscopy.

3.2. Energies, GB and PA. As can be seen from Table 3, the order in relative stability among the seven conformers should be as follows: IA ≈ IB > IIA ≈ IIB > IIIA ≈ IIIB > IV, indicating that the global minimum should be IA or IB, which is well consistent with the global minimum of alanine amide.[1] The same order in relative stability is still kept after taking the zero-point vibrational energy (ZPVE) corrections into account. The corrected energy separations relative to the global minimum are 6.28, 10.97, and 12.39 kJ/mol for conformers II, III, and IV, respectively. As mentioned above, however, Sulzbach et al. reported that the global minimum of glycine amide is located at $\psi = 165°$ (*D*(N3C2C1N4)); a second minimum (1.3 kcal/mol higher in energy) is located at 2°; the structure with $\psi = 180.0°$ has C_1 symmetry and resembles a distorted version of the global minimum. On the contrary, the global minimum should be located at $\psi = +13.84$ or $-13.93°$ in the present

TABLE 4: Calculated Proton Affinities (PA) and Gas-Phase Basicities (GB) of Glycine Amide for Three Active Sites[a,b]

active sites	IB	IIB	IIIB	IV
N3	216.81 (216.64)	218.34 (217.00)	219.46 (218.90)	219.72 (219.10)
O5	210.91 (210.79)	216.52 (214.80)	217.63 (216.71)	213.80 (213.24)
O5′	209.50 (209.19)	201.54 (200.92)	203.51 (203.73)	212.40 (211.65)
N4	197.11 (198.40)	190.93 (192.11)	191.28 (193.75)	200.01 (200.84)

[a] The units of PA(GB) are in kcal/mol. [b] O5 and O5′ refer to the PA and GB in which the proton attached to the trans- and cis- NH_2 amide, respectively.

study. The second minimum is 1.50 kcal/mol higher in energy than the global minimum, and the C_s symmetry conformer is located at not $\psi = 180.0°$ but 0.0°. From the viewpoint of the structure, the global minimum in previous studies can be comparable to conformer IIB in our studies. Apparently, the reason for this inconsistent results with ours may derive from the limitations of the RHF/6-31G* level of theory they used, without considering electron correlations and diffuse functions, because both of them are necessary for the proper descriptions of the intramolecular H-bond systems.

To further verify the relative stabilities of all the conformers, single-point energy calculations have been performed by employing the higher-level calculations including MP2, MP3, MP4SDQ, and CCSD(T) with Dunning's correlation consistent basis set aug-cc-PVDZ, respectively. The calculated results listed in Table 3 give the same order in relative energies as those of the B3LYP/6-311++G** level of theory. It should be noted that the differences between mirror-image conformers are much smaller than the expected error limits of these calculations implied in the used method and basis set. They can be regarded as meaningless physically. If we ignore the above errors implied, the consistent results between B3LYP/6-311++g** and higher-levels of theory should be confirmed. Thus the relative stabilities of the available conformers may be determined correctly at the B3LYP/6-311++g** level of theory.

As mentioned above, all the conformers have large dipole moments, ranging from 3.44 to 4.18 D, indicating that they exhibit large polar character and therefore have great affinity to polar solvent. Thus, in polar solution such as water, all the conformers are expected to be more stable than in the gas phase. This prediction has been verified by our calculations in aqueous solution employing the SCRF theory. Computational results indicate that all the conformers have been stabilized from 10.21 to 15.29 kJ/mol by the solution. The order in relative energies remains the same as in the gas phase with the exception of conformers III and IV. The reverse order between III and IV should be due to the larger dipole moment for IV (4.18 D) with respect to III (3.73 D). Another point is that the slightly larger energy differences between mirror-image conformers may be observed with respect to those in the gas phase, though they still possess mirror-image characters approximately. For example, the energy differences between IA and IB, IIA and IIB, and IIIA and IIIB are 2.82, 1.73, and 0.94 kJ/mol, respectively. Of course, placing such a system with different H-bonding strength into a cavity within a dielectric medium does not represent the realistic situation in the biological medium as suggested by Ramek et al.,[35] the more extensive theoretical investigations on glycine amide in aqueous solution are in progress.

As an important supplement in property for glycine amide, the GBs and PAs are calculated on the basis of the accurate geometries of the available conformers. As can be seen from Table 4, the most stable structures of protonated glycine amide are those in which a proton is bonded to the amino nitrogen as for the most amino acids.[37,50−53] In more detail, the PAs at O5 (O5′) and N4 sites are smaller than those of the N3 site by 3.87 (11.85) and 23.75 kcal/mol, respectively. All PAs are slightly larger than GBs except the N4 protonation, reflecting the different contributions of entropy to Gibbs free energy. The good agreement of the PA (216.81 kcal/mol) of the global minimum and the experimental value (217.73 kcal/mol)[57] has fully verified the reliability of the B3LYP/6-311++G** level of theory used here. At the same time, the PAs or GBs of the amide N and carbonyl O also play an important role in understanding the different affinity among three active sites because the experimental results on the PAs and GBs refer to the protonations of the amino groups usually.

TABLE 5: Atomic Charge Distributions for the Glycine Amide Conformers[a]

atom	IB	IIB	IIIB	IV
C1	0.66 (0.66)	0.65 (0.66)	0.67 (0.67)	0.65 (0.66)
C2	−0.27 (−0.27)	−0.27 (−0.27)	−0.26 (−0.27)	−0.28 (−0.27)
N3	−0.87 (−0.88)	−0.83 (−0.84)	−0.85 (−0.85)	−0.85 (−0.85)
N4	−0.82 (−0.81)	−0.82 (−0.80)	−0.81 (−0.80)	−0.82 (−0.80)
O5	−0.64 (−0.69)	−0.63 (−0.67)	−0.63 (−0.66)	−0.63 (−0.67)
H6	0.41 (0.42)	0.39 (0.40)	0.39 (0.40)	0.39 (0.40)
H7	0.20 (0.20)	0.20 (0.20)	0.19 (0.19)	0.22 (0.21)
H8	0.21 (0.21)	0.20 (0.20)	0.18 (0.19)	0.22 (0.21)
H9	0.36 (0.37)	0.35 (0.35)	0.35 (0.35)	0.36 (0.36)
H10	0.36 (0.38)	0.36 (0.36)	0.38 (0.37)	0.36 (0.36)
H11	0.39 (0.39)	0.40 (0.40)	0.40 (0.40)	0.40 (0.40)

[a] The data in parentheses refer to the results in aqueous solution.

Compared with protonated glycine,[50−53] the PA or GB (at N3 site) is larger than that of glycine, which is consistent with the findings of Remko.[31] Additionally, the BSSEs produced in the calculations of GBs and PAs are smaller with respect to the ZPVE corrections (about 0.51 vs 8.4 kcal/mol), indicating the importance of ZPVE corrections during the calculations of GBs and PAs.

3.3. Population Analyses and IP Discussions. Table 5 presents the natural atomic charge distributions for all the atoms in the gas phase and in aqueous solution. First, three nucleophilic active sites in glycine amide can be found, i.e., the N3, N4, and O5 site (see Figure 1). Intuitionally, the most favorable site should be N3 because it has more negative charges than N4 and O5 sites, which has been verified by the calculations of GBs and PAs. Note that the charge distributions in aqueous solution are almost identical with those in the gas phase except that the O5 site has more negative charges and the charge at N4 site decreases slightly. This observation implies that the O5 site may have higher nucleophilicity in aqueous solution. Of course, this inference from chemical intuition should be tested by future studies in aqueous solution. Second, the charge distributions also can help us explore the H-bond character qualitatively because previous studies have shown that the hydrogen atom having the H-bonding in the molecule always carries more positive charges,[54] which can also be verified by our present studies. For example: the calculated atomic charge of H6 is 0.41, higher than 0.39 over the H11 in conformer I; H11 is 0.40, higher than 0.39 over the H6 in conformer II; in conformer III, the charges of H10(0.38) and H11(0.40) are higher than those of the H9(0.35) and H6(0.39), respectively; H11 has 0.40, being higher than that of H6(0.39) for conformer IV. From the dihedral angles displayed in Figure 1, we can see that the smaller dihedral angle (less than 3°) should be favorable to form the intramolecular H-bonds because it is necessary that the lone-pair orbitals of N or O atom must have overlapped with the hydrogen orbital in a certain way.

TABLE 6: Calculated Frontier Orbital Energies (au) and Ionization Potentials (eV) for Glycine Amide Conformers at the B3LYP/6-311++G Level**

parameter	IB	IIB	IIIB	IV
ϵ_{HOMO}	−0.25128	−0.25157	−0.24678	−0.24315
ϵ_{LUMO}	−0.0235	−0.0226	−0.02195	−0.02926
$\Delta\epsilon$[a]	6.20	6.23	6.12	5.82
IP_1[b]	6.84 (9.49)	6.85 (9.50)	6.72 (9.33)	6.62 (9.20)
IP_2[c]	9.25	9.29	9.27	8.98
IP_3[c]	8.60	8.57	8.52	8.49

[a] $\Delta\epsilon$ (in eV) refers to the energy difference between the LUMO and HOMO. [b] IP_1 refers to $-\epsilon_{HOMO}$ and the data in parentheses are obtained from the linear correlations relationship in ref 59: $IP_{calc} = 1.3124(-\epsilon_{HOMO}) + 0.514$ eV. [c] IP_2 and IP_3 refer to the vertical and adiabatic ionization potential, respectively.

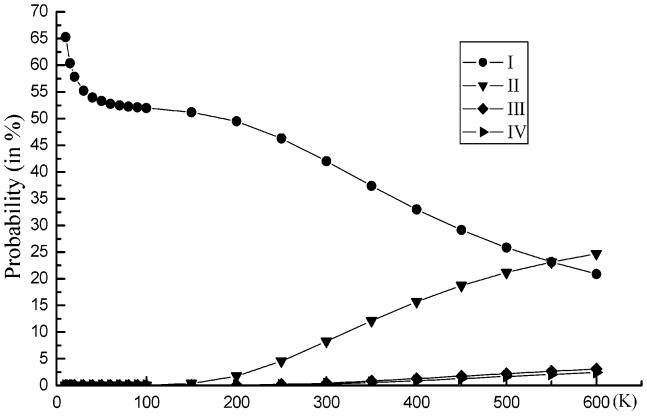

Figure 3. Equilibrium compositions of the seven conformers of glycine amide versus temperatures at 1.0 atm.

On the basis of the photoelectron spectroscopic studies on some biological molecules, Dougherty et al. pointed out that there is a linear relation between the ionization potential (IP) of the highest occupied molecular orbital (HOMO) and the biological activity.[55,56] As we all know, the IP of the HOMO is a reflection of the electron-donating ability. Namely, the smaller the IP of the HOMO is, the stronger the electron-donating ability of the molecules is. From the IPs listed in Table 6, we can know that the conformer IV possesses larger activity than other conformers because it has the smallest IP of the HOMO and the energy gap between HOMO and lowest unoccupied molecular orbital (LUMO), which has been verified by the calculated vertical and adiabatic ionization potentials. Note that there is no equivalent to Koopman's theorem; i.e., the vertical ionization potentials are not identical to the negative of the HOMO energies qualitatively, within the Kohn−Sham (KS) scheme of DFT. However, an applicable linear correlation relationship exists between the HOMO energies and the calculated vertical IPs within DFT.[58,59] As displayed in Table 6, the IPs calculated from the linear correlation are consistent with our calculated vertical IPs on the whole.

Additionally, an apparent phenomenon in the ionization process is significant elongation of the C1−C2 bond (by about 0.18 Å). This may be derived from the fact that the HOMO from which the electron is removed possesses important bonding character between both carbon atoms.

3.4. Equilibrium Distributions. Figure 3 shows how the equilibrium distribution of a conformer varies with temperatures. Obviously, the distributions of seven conformers present three different trends with increasing temperature. In more detail, the global minimum I predominates the conformational composition before 150 K. While in the range 150−600 K, compositions of conformer I decrease gradually but other conformers increase

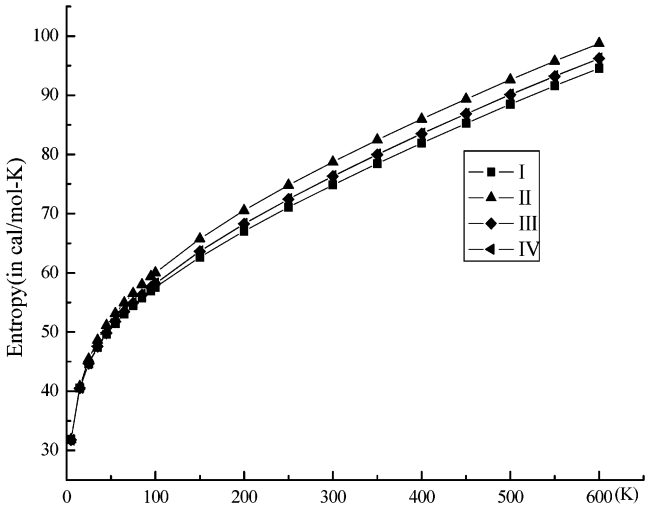

Figure 4. Dependence of entropy on temperatures at 1.0 atm.

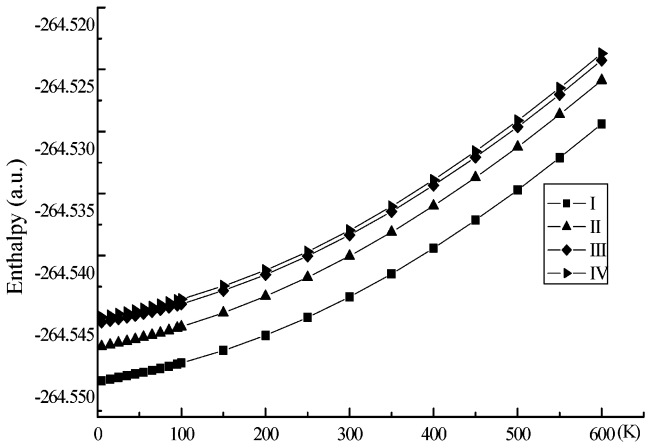

Figure 5. Dependence of enthalpy on temperatures at 1.0 atm.

when the temperature increases. More and more molecules assume the conformer II. At about 550 K, four conformers, i.e., IA, IB, IIA, and IIB, possess almost identical compositions (about 25%). Apparently, conformers III and IV make minor contributions to the equilibrium positions of glycine amide. At room temperature (about 298.15 K), the equilibrium compositions are mainly composed of conformer I and II exclusively, i.e., about 75.02% and 23.28%, respectively. These different changes may result from the changes of the entropy terms. As displayed in Figure 4, the calculated results show that the entropies of the available conformers increase with increasing temperature. However, conformer II possesses a larger entropy than others and conformer I possesses the smallest one at various temperatures. The larger entropy of conformer II may be traced to a large vibrational entropy term arising from a lower frequency ($\sim$38 cm^{-1}) with respect to other conformers as for glycine studied by Jensen et al.[8] Of course, the changes of enthalpy may also be another factor affecting the ΔG, though its influence is smaller than entropy at various temperatures as illustrated in Figure 5.

3.5. Frequencies and Infrared Intensities. Table 7 presents the calculated results of vibrational frequencies, infrared intensities, and the assignment of the different normal modes approximately. The inexistence of imaginary frequencies verifies that all the optimized structures under study correspond to minima on the PES of glycine amide. Note that the high-intensity infrared bands occur in different regions for the different conformers. For example, conformer I has intensive

TABLE 7: Frequencies (in cm^{-1}), Infrared Intensities (km/mol, in Parentheses), and Normal Mode Descriptions for Glycine Amide Conformers at the B3LYP/6-311++G Level**

freq	IB	approximate description	IIB	approximate description	IIIB	approximate description	IV	approximate description
$\nu 1$	98.8 (1.2)	τC_1C_2	41.3 (7.9)	τC_1C_2	81.2 (9.2)	τC_1C_2	76.8 (0.0)	τC_1C_2
$\nu 2$	213.0 (9.5)	$\tau N_3H_9H_{10} + \omega N_4H_6H_{11}$	167.9 (179.0)	$\omega N_4H_6H_{11} + \tau C_2N_3$	221.6 (188.0)	$\omega N_4H_6H_{11} + \rho N_3H_9H_{10}$	205.4 (242.4)	$\omega N_4H_6H_{11} + \tau N_3H_9H_{10}$
$\nu 3$	303.1 (21.1)	$\tau N_3C_2C_1N_4$	198.1 (84.3)	$\tau N_3H_9H_{10} + \tau C_2N_3$	237.3 (78.2)	$\rho N_3H_9H_{10} + \omega N_4H_6H_{11}$	278.5 (7.1)	$\tau N_3C_2C_1N_4$
$\nu 4$	383.6 (220.0)	$\omega N_4H_6H_{11} + \tau N_3H_9H_{10}$	265.3 (25.6)	$\tau N_3C_2C_1O_5 + \delta C_2C_1N_4$	289.3 (1.7)	$\tau N_3C_2C_1O_5 + \delta C_2C_1N_4$	364.1 (0.1)	$\tau N_3H_9H_{10} + \omega N_4H_6H_{11}$
$\nu 5$	501.6 (6.8)	$\rho C_2C_1O_5 + \nu C_1C_2$	436.4 (7.2)	$\delta C_2C_1N_4 + \delta N_3C_2C_1$	438.05 (4.1)	$\delta C_2C_1N_4$	494.6 (11.9)	$\nu C_1C_2 + \rho C_2C_1O_5$
$\nu 6$	527.2 (16.5)	$\delta C_1O_5N_4 + \delta C_1C_2N_3$	487.5 (9.3)	$\tau C_2N_3 + \tau N_4H_6H_{11}$	505.2 (11.0)	$\omega C_1O_5N_4 + \rho C_2H_7H_8$	507.2 (8.3)	$\rho C_2H_7H_8 + \tau N_4H_6H_{11} + \rho N_3H_9H_{10}$
$\nu 7$	580.5 (10.4)	$\delta C_1C_2N_3 + \delta C_1O_5N_4$	617.6 (5.7)	$\tau N_4H_6H_{11} + \rho C_2H_7H_8 + \delta N_3C_2C_1 + \delta C_1O_5N_4$	598.1 (7.7)	$\tau N_3C_2C_1O_5 + \tau N_4H_6H_{11}$	515.6 (42.5)	$\delta C_1O_5N_4 + \delta C_1C_2N_3$
$\nu 8$	707.0 (2.3)	$\tau N_4H_6H_{11} + \rho C_2H_7H_8$	641.5 (2.9)	$\tau N_3C_2C_1O_5 + \rho C_2H_7H_8 + \delta C_1O_5N_4 + \tau N_4H_6H_{11}$	673.8 (12.0)	$\tau N_3C_2C_1O_5 + \omega C_1O_5N_4$	656.4 (11.1)	$\tau N_4H_6H_{11} + \rho C_2H_7H_8$
$\nu 9$	804.1 (63.9)	$\nu C_1C_2 + \omega N_3H_9H_{10}$	787.8 (36.3)	$\nu C_1C_2 + \rho N_4H_6H_{11}$	812.5 (4.5)	$\nu C_1C_2 + \rho N_4H_6H_{11}$	671.3 (221.7)	$\omega N_3H_9H_{10} + \delta C_1O_5N_4 + \delta C_1C_2N_3$
$\nu 10$	869.3 (64.8)	$\rho C_2H_7H_8 + \tau N_3H_9H_{10} + \nu C_1C_2$	915.1 (145.5)	$\omega N_3H_9H_{10} + \rho C_2H_7H_8 + \nu C_2N_3$	842.0 (159.9)	$\nu C_2N_3 + \omega N_3H_9H_{10} + \rho C_2H_7H_8$	837.1 (14.0)	$\nu C_1C_2 + \nu C_1N_4$
$\nu 11$	957.0 (36.3)	$\rho C_2H_7H_8 + \tau N_3H_9H_{10}$	919.3 (23.8)	$\tau N_3H_9H_{10} + \tau C_2H_7H_8 + \nu C_2N_3$	1014.4 (13.0)	$\rho C_2H_7H_8 + \nu C_2N_3 + \omega C_1O_5N_4$	900.4 (1.8)	$\rho C_2H_7H_8 + \tau N_3H_9H_{10}$
$\nu 12$	1071.6 (21.8)	$\nu C_2N_3 + \rho N_4H_6H_{11}$	1077.6 (6.9)	$\nu C_1N_4 + \nu C_2N_3 + \rho N_4H_6H_{11}$	1084.6 (5.4)	$\nu C_1N_4 + \nu C_2N_3 + \rho N_4H_6H_{11}$	1068.4 (4.8)	$\rho N_4H_6H_{11} + \nu C_1N_4 + \nu C_1O_5$
$\nu 13$	1100.6 (3.3)	$\rho N_4H_6H_{11} + \nu C_1N_4$	1143.9 (8.0)	$\nu C_2N_3 + \rho N_4H_6H_{11}$	1109.7 (8.8)	$\nu C_2N_3 + \rho N_4H_6H_{11}$	1111.7 (27.5)	νC_2N_3
$\nu 14$	1171.2 (0.6)	$\tau C_2H_7H_8 + \tau N_3H_9H_{10}$	1178.0 (2.2)	$\tau C_2H_7H_8 + \tau N_3H_9H_{10} + \nu C_2N_3$	1205.6 (13.8)	$\nu C_2N_3 + \rho N_4H_6H_{11} + \tau N_3H_9H_{10}$	1169.3 (0.1)	$\tau C_2H_7H_8 + \tau N_3H_9H_{10}$
$\nu 15$	1317.6 (27.9)	$\tau C_2H_7H_8 + \tau N_3H_9H_{10} + \nu C_1C_2 + \nu C_1N_4$	1286.9 (140.5)	$\nu C_1N_4 + \omega C_2H_7H_8$	1254.8 (2.4)	$\tau C_2H_7H_8 + \nu C_2N_3 + \tau N_3H_9H_{10}$	1340.1 (121.3)	$\nu C_1N_4 + \delta C_1N_4H_{11} + {}_{\nu C_1}C_2$
$\nu 16$	1354.3 (57.7)	$\omega C_2H_7H_8 + \nu C_1N_4$	1381.3 (15.8)	$\omega C_2H_7H_8 + \nu C_1C_2 + \nu C_1N_4 + \tau N_3H_9H_{10}$	1321.8 (148.9)	$\nu C_1N_4 + \omega C_2H_7H_8 + \tau N_3H_9H_{10}$	1360.6 (25.1)	$\omega C_2H_7H_8 + \nu C_1N_4$
$\nu 17$	1387.9 (29.5)	$\omega C_2H_7H_8 + \nu C_1C_2 + \tau N_3H_9H_{10} + \nu C_1N_4$	1396.3 (7.2)	$\omega C_2H_7H_8 + \nu C_1C_2 + \nu C_1N_4 + \tau N_3H_9H_{10}$	1439.5 (26.2)	$\omega C_2H_7H_8 + \nu C_1C_2 + \nu C_1N_4 + \tau N_3H_9H_{10}$	1369.7 (0.2)	$\tau C_2H_7H_8 + \tau N_3H_9H_{10}$
$\nu 18$	1477.2 (5.21)	$\delta C_2H_7H_8$	1469.1 (7.5)	$\delta C_2H_7H_8$	1497.1 (6.9)	$\delta C_2H_7H_8$	1456.8 (3.3)	$\delta C_2H_7H_8$
$\nu 19$	1583.8 (150.3)	$\delta N_4H_6H_{11}$	1620.6 (89.6)	$\delta N_4H_6H_{11}$	1620.6 (64.2)	$\delta N_4H_6H_{11} + \delta N_3H_9H_{10}$	1602.1 (117.1)	$\delta N_4H_6H_{11}$
$\nu 20$	1665.1 (37.4)	$\delta N_3H_9H_{10}$	1682.3 (23.6)	$\delta N_3H_9H_{10}$	1640.8 (135.5)	$\delta N_3H_9H_{10} + \delta N_4H_6H_{11}$	1660.2 (24.7)	$\delta N_3H_9H_{10}$
$\nu 21$	1763.1 (418.1)	νC_1O_5	1765.7 (354.1)	νC_1O_5	1769.0 (314.0)	νC_1O_5	1757.6 (376.0)	νC_1O_5
$\nu 22$	3028.3 (26.4)	$\nu_s C_2H_7H_8$	3018.2 (31.4)	$\nu_s C_2H_7H_8$	2945.2 (54.0)	$\nu_s C_2H_7H_8$	3052.9 (13.6)	$\nu_s C_2H_7H_8$
$\nu 23$	3077.4 (9.5)	$\nu_{as} C_2H_7H_8$	3056.3 (17.3)	$\nu_{as} C_2H_7H_8$	3026.0 (39.0)	$\nu_{as} C_2H_7H_8$	3089.1 (6.8)	$\nu_{as} C_2H_7H_8$
$\nu 24$	3519.5 (1.4)	$\nu_s N_3H_9H_{10}$	3503.9 (2.5)	$\nu_s N_3H_9H_{10}$	3500.0 (10.9)	$\nu_s N_3H_9H_{10}$	3536.9 (1.8)	$\nu_s N_3H_9H_{10}$
$\nu 25$	3564.4 (46.8)	$\nu_s N_4H_6H_{11}$	3572.3 (6.0)	$\nu_{as} N_3H_9H_{10}$	3589.3 (39.4)	$\nu_s N_4H_6H_{11}$	3592.4 (28.7)	$\nu_s N_4H_6H_{11}$
$\nu 26$	3597.9 (7.6)	$\nu_{as} N_3H_9H_{10}$	3586.3 (32.9)	$\nu_s N_4H_6H_{11}$	3592.8 (13.4)	$\nu_{as} N_3H_9H_{10}$	3631.7 (7.6)	$\nu_{as} N_3H_9H_{10}$
$\nu 27$	3708.8 (83.4)	$\nu_{as} N_4H_6H_{11}$	3716.6 (39.8)	$\nu_{as} N_4H_6H_{11}$	3720.6 (43.3)	$\nu_{as} N_4H_6H_{11}$	3723.5 (55.5)	$\nu_{as} N_4H_6H_{11}$

bands at 383.6, 1583.8, and 1763 cm^{-1}; II at 167.9, 915.1, 1286.9, and 1765.7 cm^{-1}; III at 221.6, 842.0, 1321.8, 1640.8, and 1769.0 cm^{-1}; and IV at 205.4, 671.3, 1340.1, 1602.1, and 1757.6 cm^{-1}, respectively. These bands should provide some help in the identification of them by means of the gas-phase vibrational spectrum. Obviously, the most characteristic band among all the conformers is the C═O stretching vibration, which is at about 1757−1769 cm^{-1}.

As displayed in Table 7, the pure stretching modes, corresponding to the four highest harmonic vibrational frequencies, contain additional information about the formations of the different strength of H-bonds. From the order of the symmetric or asymmetric stretching vibrations of two different $-NH_2$ terminals, the red shifts take place in all the conformers except conformer II due to the formations of the intramolecular H-bonds. Moreover, the larger red shifts in conformer I with respect to other conformers (about 25 cm^{-1}) indicate that the intramolecular H-bond formed from the amide to the amine should be the strongest one. For two $-NH_2$ terminals, the bands attributed to the N−H bending vibrations (ν19 and ν20) are more intensive than the corresponding stretching vibrations (from ν24 to ν27). Furthermore, the higher intensive absorption for amide than amine regardless of whether stretching vibrations or bending vibrations should provide the best spectrum proof of the identification of them. Additionally, the lower frequency of II (from ν1 to ν6) with respect to other conformers should be responsible for its large entropy terms mentioned above.

Inspection of the vibrational frequencies in aqueous solution, we can observe that the vibrational modes in the gas phase do not change nearly. Thus, those analyses in the gas phase should also be applied to the situation in aqueous solution.

4. Conclusions

Accurate geometries, relative energies, rotational constants, dipole moments, harmonic vibrational frequencies and their corresponding infrared intensities have been determined for the seven conformers of neutral glycine amide in the gas phase and in aqueous solution, employing the B3LYP/6-311++G** level of theory. Among the seven conformers, three pairs of mirror-image conformers and one C_s symmetry conformer have been found. Higher level computations, including the MP2, MP3, MP4SDQ, and CCSD(T) methods with Dunning's correlation consistent basis set aug-cc-PVDZ, indicate that the global minimum should be conformer I regardless of whether in the gas phase or in aqueous solution, which is different from the previous theoretical reports.[33] The intramolecular H-bond formed from the amide to the amine plays a key role in stabilizing the global minimum as observed in alanine amide and has been discussed qualitatively from the viewpoint of the structures, charge distributions and vibrational analyses. On the basis of the accurate geometries of the available minima, the GBs and PAs have also been determined and the PA of the global minimum is very consistent with the experimental value. Moreover, the equilibrium distributions for the seven conformers have been predicted using the relative Gibbs free energy. At room temperature, the equilibrium compositions are mainly composed of conformers I and II exclusively, i.e., about 75.02% and 23.28%, respectively. Those frequency analyses should allow interpretation of a carefully executed experimental investigation of the gas-phase vibrational spectrum of glycine amide, as suggested by Császár when studying glycine.[10] Additionally, the results, such as vertical and adiabatic ionization potentials, rotational constants, and dipole moments, should also be useful to experimentalists.

Acknowledgment. This work is supported by the National Natural Science Foundation of China (20273040, 29973022) and the Foundation for University Key Teacher by the Ministry of Education of China. We are also grateful to Dr. Milan Remko and Michael Ramek for their valuable correspondences, and to the referees for their excellent suggestions to improve presentation of the results.

References and Notes

(1) Lavrich, R. J.; Farrar, J. O.; Tubergen, M. J. *J. Phys. Chem. A* **1999**, *103*, 4659.
(2) Vishveshwara, S.; Pople, J. A. *J. Am. Chem. Soc.* **1977**, *99*, 2422.
(3) Tse, Y.-C.; Newton, M. D.; Vishveshwara, S.; Pople, J. A. *J. Am. Chem. Soc.* **1978**, *100*, 4329.
(4) Sellers, H. L.; Schäfer, L. *J. Am. Chem. Soc.* **1978**, *100*, 7728.
(5) Schäfer, L.; Sellers, H. L.; Lovas, F. J.; Suenram, R. D. *J. Am. Chem. Soc.* **1980**, *102*, 6566.
(6) Wright, L. R.; Borkman, R. F. *J. Am. Chem. Soc.* **1980**, *102*, 6207.
(7) Bonaccorsi, R.; Palla, P.; Tomasi, J. *J. Am. Chem. Soc.* **1984**, *106*, 1945.
(8) Jensen, J. H.; Gordon, M. S. *J. Am. Chem. Soc.* **1991**, *113*, 7917.
(9) Yu, D.; Armstrong, D. A.; Rauk, A. *Can. J. Chem.* **1992**, *70*, 1762.
(10) Császár, A. G. *J. Am. Chem. Soc.* **1992**, *114*, 9568.
(11) Hu, C.-H.; Shen, M.; Schaefer, H. F., III. *J. Am. Chem. Soc.* **1993**, *115*, 2923.
(12) Barone, V.; Adamo, C.; Lelj, F. *J. Chem. Phys.* **1995**, *102*, 364.
(13) Császár, A. G. *J. Mol. Struct. (THEOCHEM)* **1995**, *346*, 141.
(14) Yu, D.; Rauk, A.; Armstrong, D. A. *J. Am. Chem. Soc.* **1995**, *117*, 1789.
(15) Godfrey, P. D.; Brown, R. D. *J. Am. Chem. Soc.* **1995**, *117*, 2019.
(16) Sirois, S.; Proynov, E. I.; Nguyen, D. T.; Salahub, D. R. *J. Chem. Phys.* **1997**, *107*, 6770.
(17) Nguyen, D. T.; Scheiner, A. C.; Andzelm, J. W.; Sirois, S.; Salahub, D. R.; Hagler, A. T. *J. Comput. Chem.* **1997**, *18*, 1609.
(18) Chakraborty, D.; Manogaran, S. *Chem. Phys. Lett.* **1998**, *294*, 56.
(19) Tortonda, F. R.; Pascual-Ahuir, J. L.; Silla, E.; Tuñón, I.; Ramírez, F. J. *J. Chem. Phys.* **1998**, *109*, 592.
(20) Stepanian, S. G.; Reva, I. D.; Radchenko, E. D.; Rosado, M. T. S.; Duarte, M. L. T. S.; Fausto, R.; Adamowicz, L. *J. Phys. Chem. A* **1998**, *102*, 1041.
(21) Kaschner, R.; Hohl, D. *J. Phys. Chem. A* **1998**, *102*, 5111.
(22) Chaban, G. M.; Jung, J. O.; Gerber, R. B. *J. Phys. Chem. A* **2000**, *104*, 10035.
(23) Rodríguez-Santiago, L.; Sodupe, M.; Oliva, A.; Bertran, J. *J. Phys. Chem. A* **2000**, *104*, 1256.
(24) Gutowski, M.; Skurski, P.; Simons, J. *J. Am. Chem. Soc.* **2000**, *122*, 10159.
(25) Pacios, L. F.; Gálvez, O.; Gómez, P. C. *J. Phys. Chem. A* **2001**, *105*, 5232.
(26) Pacios, L. F.; Gómez, P. C. *J. Comput. Chem.* **2001**, *22*, 702.
(27) Oie, T.; Loew, G. H.; Burt, S. K.; MacElroy, R. D. *J. Am. Chem. Soc.* **1984**, *106*, 8007.
(28) Jensen, J. H.; Baldridge, K. K.; Gordon, M. S. *J. Phys. Chem.* **1992**, *96*, 8340.
(29) Császár, A. G. *J. Phys. Chem.* **1996**, *100*, 3541.
(30) Remko, M.; Rode, B. M. *Chem. Phys. Lett.* **2000**, *316*, 489.
(31) Remko, M.; Rode, B. M. *Phys. Chem. Chem. Phys.* **2001**, *3*, 4667.
(32) Klassen, J. S.; Kebarle, P. *J. Am. Chem. Soc.* **1997**, *119*, 6552.
(33) Sulzbach, H. M.; Schleyer, P. V. R.; Schaefer, H. F., III. *J. Am. Chem. Soc.* **1994**, *116*, 3967.
(34) Ramek, M.; Cheng, V. K. W. *Int. J. Quantum Chem., Quantum Boil. Symp.* **1992**, *19*, 15.
(35) Remko, M.; Walsh, O. A.; Richards, W. G. *Chem. Phys. Lett.* **2001**, *336*, 156.
(36) Stepanian, S. G.; Reva, I. D.; Radchenko, E. D.; Adamowicz, L. *J. Phys. Chem. A* **1998**, *102*, 4623.
(37) Topol, I. A.; Burt, S. K.; Toscano, M.; Russo, N. *J. Mol. Struct. (THEOCHEM)* **1998**, *430*, 41.
(38) Frisch, M. J.; Pople, J. A.; Del Bene, J. E. *J. Phys. Chem.* **1985**, *89*, 3664.
(39) Bene, J. E. D.; Jordan, M. J. T. *J. Mol. Struct. (THEOCHEM)* **2001**, *573*, 11.
(40) Becke, A. D. *J. Chem. Phys.* **1993**, *98*, 5648.
(41) Lee, C.; Yang, W.; Parr, R. G. *Phys. Rev. B* **1988**, *37*, 785.
(42) Boys, S. F.; Bernardi, F. *Mol. Phys.* **1970**, *19*, 553.
(43) Wong, M. W.; Frisch, M. J.; Wiberg, K. B. *J. Am. Chem. Soc.* **1991**, *113*, 4776.
(44) Wong, M. W.; Wiberg, K. B.; Frisch, M. J. *J. Am. Chem. Soc.* **1992**, *114*, 523.

(45) Wong, M. W.; Wiberg, K. B.; Frisch, M. J. *J. Chem. Phys.* **1991**, *95*, 8991.

(46) Wong, M. W.; Wiberg, K. B.; Frisch, M. J. *J. Am. Chem. Soc.* **1992**, *114*, 1645.

(47) Frisch, M. J.; Trucks, G. W.; Schlegel, H. B.; Scuseria, G. E.; Robb, M. A.; Cheeseman, J. R.; Zakrzewski, V. G.; Montgomery, J. A., Jr.; Stratmann, R. E.; Burant, J. C.; Dapprich, S.; Millam, J. M.; Daniels, A. D.; Kudin, K. N.; Strain, M. C.; Farkas, O.; Tomasi, J.; Barone, V.; Cossi, M.; Cammi, R.; Mennucci, B.; Pomelli, C.; Adamo, C.; Clifford, S.; Ochterski, J.; Petersson, G. A.; Ayala, P. Y.; Cui, Q.; Morokuma, K.; Malick, D. K.; Rabuck, A. D.; Raghavachari, K.; Foresman, J. B.; Cioslowski, J.; Ortiz, J. V.; Stefanov, B. B.; Liu, G.; Liashenko, A.; Piskorz, P.; Komaromi, I.; Gomperts, R.; Martin, R. L.; Fox, D. J.; Keith, T.; Al-Laham, M. A.; Peng, C. Y.; Nanayakkara, A.; Gonzalez, C.; Challacombe, M.; Gill, P. M. W.; Johnson, B.; Chen, W.; Wong, M. W.; Andres, J. L.; Gonzalez, C.; Head-Gordon, M.; Replogle, E. S.; Pople, J. A. Gaussian98, revision X.X; Gaussian, Inc.: Pittsburgh, PA, 1998.

(48) Branden, C.; Tooze, J. *Introduction to Protein Structure*; Garland Publishing: New York, 1991.

(49) Lundell, J.; Krajewska, M.; Räsänen, M. *J. Phys. Chem. A* **1998**, *102*, 6643.

(50) Zhang, K.; Chung-Phillips, A. *J. Phys. Chem. A* **1998**, *102*, 3625.

(51) Zhang, K.; Chung-Phillips, A. *J. Comput. Chem.* **1998**, *19*, 1862.

(52) Noguera, M.; Rodríguez-Santiago, L.; Sodupe, M.; Bertran, J. *J. Mol. Struct. (THEOCHEM)* **2001**, *537*, 307.

(53) Maksić, Z. B.; Kovačević, B. *Chem. Phys. Lett*. **1999**, *307*, 497.

(54) Zhu, H.-S.; Ho, J.-J. *J. Phys. Chem. A* **2001**, *105*, 6543.

(55) Dougherty, D.; Younathan, E. S.; Voll, R.; Abdulnur, S.; McGlynn, S. P. *J. Electron Spectrosc. Relat. Phenom.* **1978**, *13*, 379.

(56) Jiang, P.; Qian, X.; Li, C.; Qiao, C.; Wang, D. *Chem. Phys. Lett.* **1997**, *277*, 508.

(57) Kinser, R. D.; Ridge, D. P.; Hvistendahl, G.; Rasmussen, B.; Uggerud, E. *Chem. Eur. J.* **1996**, *2*, 1143.

(58) Stowasser, R.; Hoffmann, R. *J. Am. Chem. Soc.* **1999**, *121*, 3414.

(59) Zhan, C.-G.; Nichols, J. A.; Dixon, D. A. *J. Phys. Chem. A* **2003**, *107*, 4184.